Pergamon

*Int. J. Heat Mass Transfer.* Vol. 40, No. 12, pp. 2813–2823, 1997

Printed in Great Britain
0017–9310/97 $17.00 + 0.00

PII: S0017–9310(96)00336–5

# Effects of leading-edge roughness on fluid flow and heat transfer in the transitional boundary layer over a flat plate

MARK W. PINSON and TING WANG†

Department of Mechanical Engineering, Clemson University, Clemson, SC 29634-0921, U.S.A.

(*Received* 15 *February* 1996 *and in final form* 16 *September* 1996)

**Abstract**—An experimental study was undertaken to gain insight into the physical mechanisms that affect the laminar-turbulent transition process downstream of the leading-edge roughness condition. Sandpaper strips and small cylinders were attached to the leading edge of a heated test surface to simulate leading edge roughness typical of gas turbine blades. The roughness Reynolds numbers ranged from 2 to 2840. For free-stream velocities less than 5 m $s^{-1}$, the maximum roughness height was the primary contributor to deviations from the undisturbed case, irrespective of the roughness geometry. At higher free-stream velocities (5–7 m $s^{-1}$), three of the rough leading-edge conditions induced a dual-slope region between the laminar and turbulent Stanton number correlations. Boundary layer measurements indicated that the first segment of the dual-slope was laminar, but the wall heat transfer significantly deviates from the laminar correlation. The second segment was transitional. The dual-slope behaviour and a waviness in the Stanton number distribution observed at higher free-stream velocities are believed to have been caused by nonlinear amplification caused by the finite disturbances at the leading edge. © 1997 Elsevier Science Ltd.

## INTRODUCTION

The raising of operating temperatures to increase overall turbine efficiency has led to the need for accurate assessment of thermal loads in the turbine. Turbine blades experience significant thermal loading, and Mayle [1] and Hodson *et al.* [2] indicated that it is common for over half of the flow surrounding the turbine blades to experience laminar-turbulent transition, particularly in low pressure turbines. A better understanding of the physical mechanisms involved in the transition process is therefore desirable so that a more accurate assessment of the turbine blade temperature variations can be made possible through improved models of transitional heat transfer.

Of the many factors that can influence laminar-turbulent transition, the effect of leading-edge roughness on the process has not been clearly determined, particularly with regard to heat transfer behavior. Surface roughness can be significant to turbine vanes and blades in many ways, especially in a high pressure turbine. A study by Taylor [3] that measured the surface roughness characteristics of two used (i.e., blade surfaces had been degraded as a result of "in-service" use) turbine blades indicated the following:

(1) Roughness is usually greatest at the leading edge of the blade.
(2) Roughness consists of a relatively uniform distribution with a few isolated peaks, according to a statistical analysis.

The second observation made in Taylor's study was based on the large positive value of kurtosis ($\sim 10$; a zero value represents a Gaussian distribution) found in the study. Such large values of kurtosis indicate that the structure of the roughness samples used in the study tended to have a few isolated peaks.

Roughness can also be significant to new turbine blades because a coating may have been added to the blade to enhance its life characteristics by increasing resistance to erosion and high temperatures. The addition of the coating to the blade can leave the surface significantly rougher than an uncoated blade. Boynton *et al.* [4] demonstrated that the overall efficiency of a turbine with new spray-coated blading (10.16 $\mu$m rms roughness) was 2.1 percentage points lower than when polished blading was used (0.76 $\mu$m rms roughness). Blair [5] also showed that increasing the surface roughness by an order of magnitude doubled the heat transfer between the flow and the blades. Also, unnecessary design constraints may be imposed as safety factors to anticipate the unknown effects of roughness. The characteristics of leading-edge roughness described by Taylor and the unknown effects of

† Author to whom correspondence should be addressed.

## NOMENCLATURE

FSTI free-stream turbulence intensity
$K$ acceleration parameter $= \frac{\nu}{U_\infty^2}\frac{dU_\infty}{dx}$
LEC leading-edge condition
$Pr$ Prandtl number
$Re_1$ $Re_x$ marking the onset of dual-slope behavior in the $St$ distribution
$Re_2$ $Re_x$ marking the onset of the second slope in the dual-slope $St$ behavior
$Re_x$ local Reynolds number $= U_\infty x/\nu$
$St$ local Stanton number
$U_\infty$ free-stream velocity
$U^+$ $U/u_\tau$
$u'$ RMS streamwise velocity fluctuation
$u_\tau$ friction velocity, $\sqrt{\tau_w/\rho}$
$\overline{uv}$ time-averaged Reynolds shear stress
$\overline{vt}$ time-averaged Reynolds cross-stream heat flux
$x$ streamwise distance from the leading edge of the heated test surface
$X_{UHSL}$ streamwise unheated starting length (2.5 cm for this study)
$y$ coordinate normal to test surface
$Y^+$ $yU_\tau/\nu$.

Greek symbols
$\delta$ boundary layer thickness at $0.995U_\infty$
$\delta^*$ displacement thickness $= \int_0^\delta \left(1 - \frac{U}{U_\infty}\right) dy$
$\rho$ density
$\tau_w$ shear stress on the test surface
$\nu$ kinematic viscosity.

gas turbine blade roughness on fluid mechanics and heat transfer suggest the need to understand the influence of leading-edge roughness on transitional heat transfer behavior.

Early work on the relationship between roughness and transition has been concerned with the location of the onset of transition, usually defined by using flow visualization or by a sudden change in the total pressure near the test surface as the maximum roughness height changes. Fage and Preston [6] reported that as roughness height increased, the transition point moved progressively closer to the physical location of the roughness element disturbing the flow. Dryden [7] suggested that roughness elements tend to destabilize the boundary layer flow and that there may be a connection between the instability induced by the roughness element and classical stability theory. Klebanoff and Tidstrom [8] examined the possible connection to stability theory. Their results indicated that the presence of roughness elements in the laminar region of the boundary layer magnified the amplitude of the Tollmien–Schlichting oscillations present in the early transitional boundary layer. However, the region of frequencies amplified were still within the range of Tollmien–Schlichting wave frequencies predicted by linear stability theory.

Many studies detailing the response of the momentum boundary layer to changes in surface roughness have been conducted, but they have been limited to the response of the fully turbulent boundary layer to surface perturbations. The study performed by Jacobs [9] indicated that while velocity profiles responded slowly to a change in surface roughness, a distinct change in velocity profile was noted. Klebanoff and Diehl [10] showed that different kinds of roughness covering the initial portion of an otherwise smooth test surface produced different boundary layer structures on the surface downstream of the roughness. If sandpaper roughness was used, the velocity profiles gradually reattained self-similar behavior and the energy spectra indicated a boundary layer flow very close to that of a turbulent boundary layer formed due to natural transition. However, if spanwise cylinders were used to disturb the flow, the velocity profiles required a much greater streamwise distance to achieve self-similar behavior, and the energy spectra indicated a concentration of energy in the lower frequency range.

Other studies by Antonia and Luxton [11, 12] and Androepoulos and Wood [13] suggested that boundary layer flow responds to a change in the surface roughness in a gradual progression from the near-wall region that eventually expands to cover the entire thickness of the layer. The growth of the inner layer was observed through variations in normalized velocity profiles. Antonia and Luxton suggested that the presence of the inner layer made local similarity inapplicable, based on the results of a turbulent kinetic energy balance.

Studies of heat transfer behavior resulting from surface roughness characteristics have been examined, but, as before, the studies have been limited to the fully turbulent flow regime. Ligrani *et al.* [14] and Taylor *et al.* [15] obtained similar results of increasing heat transfer with increasing roughness, and a more recent study by Taylor *et al.* [16] showed that a step change from a rough surface to a smooth one causes a reduction in heat transfer. The Stanton number downstream of the change to a smooth surface initially decreases to a value below the smooth-wall value; then the values asymptotically recover the smooth wall values.

The addition of rough-surface coatings to new gas turbine blades and the observed nature of roughness on used gas turbine blades suggests the need for an investigation of surface roughness effects on turbine blade heat transfer. The significant region of transitional flow surrounding the rough turbine blades and the apparent lack of detailed information regarding heat transfer over rough surfaces also suggest that experimental work in this area will contribute to the overall effort to understand heat transfer around turbine blades.

The effect of leading-edge roughness on an actual gas turbine blade is undoubtedly a function of the shape of the blade (leading-edge curvature) and the gas turbine environment (high turbulence intensity, strong acceleration, film cooling etc.). In order to fundamentally understand the leading-edge effect on flow structure and heat transfer, this study focuses on flat plate roughness. The other parameters will be considered later. Hence, this study may not be directly applicable to gas turbine design, but it has the potential for improving the understanding of the roughness effect on heat transfer in the more complicated environment of the gas turbine.

## EXPERIMENTAL PROGRAM

*Test facility*

The test facility used is an open circuit, blowing-type wind tunnel [see Fig. 1(a)]. Air enters the system by passing through a filter designed to remove all particulate larger than 5 $\mu$m. A honeycomb passage is used to straighten the flow and a heat exchanger which is used to control the steadiness of the free-stream air temperature to within 0.5°C. Suction is employed upstream of the test surface to facilitate the formation of a boundary layer from zero thickness at the elliptic leading edge. The test section is a channel that measures 2.4 m in the streamwise ($x$) direction, 0.92 m in the spanwise ($z$) direction (parallel to the leading edge), and 0.15 m in the cross-stream ($y$) direction (moving away from the heated test surface). The spanwise to cross-stream ratio of 6 was determined to be sufficient to generate an approximately two-dimensional (2-D) boundary layer along the centerline of the 0.92 by 2.4 m test surface. Measurements made by Keller [17] with the test facility indicated that laminar and turbulent portions of the boundary layer were uniform 20 cm above and below the test surface centerline in the spanwise direction. The three-dimensionality of the transition portion reduced the spanwise uniformity to 8 cm above and below the centerline. For the purposes of the current study all measurements on the surface and within the boundary layer were made along the centerline of the test surface.

The test surface is a composite design consisting of several layers [see Fig. 1(c)]. Each of the layers shown in Fig. 1(c) is uniform and continuous over the entire area of the test surface. The foil heater, custom-

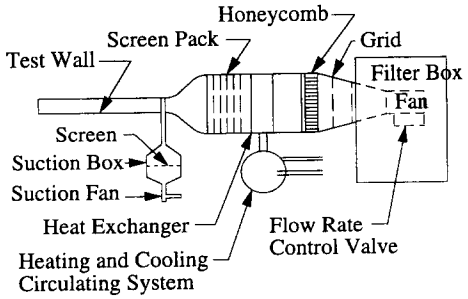


(a)

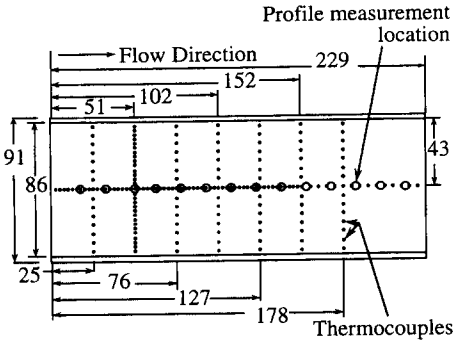


Dimensions in centimeters

(b)

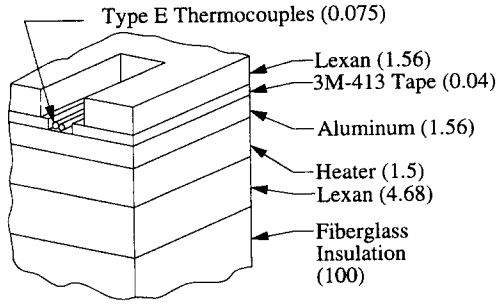


Dimensions in millimeters

(c)

Fig. 1. (a) Wind tunnel test facility; (b) thermocouple locations on heated test wall; (c) cross-section of heated test surface.

designed by Electrofilm Inc., has heating elements covering 90% of the heater surface area. The foil heating element is covered by a silicon rubber coating with a 1.56 mm sheet of aluminum vulcanized to one side. A layer of 3M-413 tape attached to the other side of the aluminum sheet contains 184 E-type thermocouples (bead diameter: 0.076 mm) distributed over the entire test surface, as shown in Fig. 1(b). The thermocouple beads are positioned such that they are in contact with the inner side of a 1.56 mm Lexan sheet. The outer side of the Lexan forms the outer layer of the test surface, which is in contact with the free-stream air within the test section. The quality of the surface smoothness was that of the standard

smoothness for commercially available, optically clear Lexan. The other side of the foil heater is supported by a 4.68 mm Lexan sheet which, in turn, is insulated with 30 cm of R-30 fiberglass.

The 2.4 by 0.92 m channel wall opposite the heated test surface is flexible to allow for adjustment of the streamwise pressure gradient. For the purposes of this study, this "outer wall" was adjusted to accommodate the growth of the boundary layer so that the streamwise pressure coefficient varied less than 1%. In addition, the outer wall contains fourteen holes (2.54 cm in diameter) along the centerline, as shown in Fig. 1. The first hole, called station 1, is located 20 cm from the leading edge of the test surface, and subsequent holes or stations are spaced 15 cm from each other. These stations permit the structure of the boundary layer to be measured as it develops in the streamwise direction. Additional information concerning the design of the wind tunnel and the composite heated test surface is provided in Kuan [18] and Zhou [19].

*Roughness conditions*

Taylor's [3] study indicated that the leading edge of a gas turbine blade is usually the roughest area of the blade and that the rough regions contain isolated peaks. Based on these results, the present study used a sandpaper strip placed at the leading edge of the test surface to simulate the roughened leading-edge condition. The strips of sandpaper were 5 cm long in the streamwise direction and covered the entire spanwise length of the leading edge. The isolated peak nature of the roughness was investigated separately, using cylinders placed at the leading edge. Only one cylinder was attached to the leading edge at a time, and like the sandpaper strips, the cylinder length spanned the entire leading edge.

To determine the appropriate scale of the leading-edge roughness and the appropriate free-stream velocity in the test section, information concerning these parameters in gas turbine engines was obtained. Taylor's [3] measurements, using two types of turbine blades, indicated roughness heights between 1.46 and 10.7 $\mu$m. Elovic [20] suggested a roughness range from 1.32 to 12.7 $\mu$m and also a unit Reynolds number, $U/\nu$, of $2.76 \times 10^7$ m$^{-1}$ as being typical around a turbine blade. A detailed study involving measurements on 58 used blades (from both military and civilian aircraft) conducted by Tarada [21] indicated roughness values ranging from 2 to 161 $\mu$m. Using the unit Reynolds number provided by Elovic and the reported roughness values, a range in roughness Reynolds number was established and is shown in Fig 2. Also shown in Fig. 2 are the grain sizes of the sandpaper strips (in grains per linear inch–GRIT or number of grains per 25.4 mm) and the cylinder diameters (in inches i.e. 0.030 = 0.030 in = 0.762 mm) used to conduct this study. The range in roughness Reynolds number shown for the cylinders and sandpaper was determined by using the maximum (19.5 m s$^{-1}$) and minimum (2.87 m s$^{-1}$) free-stream velocities obtained in the test facility.

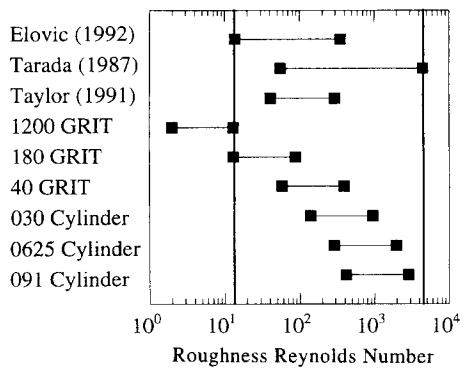


Fig. 2. Representative roughness Reynolds numbers of blades from in-service engines and the range covered by the present study.

A simple model was used to estimate the average roughness height of the sandpaper. The GRIT specification was used as an indicator of roughness height. For example, the 1200 GRIT sandpaper specification suggests that each grain is approximately 21.2 $\mu$m in length. Assuming that each grain is hemispherical and that the backing paper is completely covered with grains, the height of each particle is half the length, or 10.6 $\mu$m in this case. This method of height estimation was used for all of the sandpaper cases shown in Fig. 2. The cylinder diameters were directly measured using a micrometer.

Elmer's all-purpose glue was used to attach the cylinders to the leading edge of the plate. The bead was evenly distributed underneath the cylinder on the side closest to the leading edge. A strip of double-sided tape was used to attach the sandpaper strips to the leading-edge of the plate. Consideration of the sandpaper/double-sided tape combination suggested that the bluff shape of the tape and the sandpaper backing might influence the results in such a way as to obscure the effect of the actual grain roughness of the sandpaper. Hence, specific tests with this bluff-body leading-edge condition were added to the test pattern by attaching a single-sided strip of tape 5 cm long in the streamwise direction with a cross-stream height of 0.5 mm. The eight leading-edge conditions are summarized in Table 1.

Table 1. List of leading edge conditions

| Condition | Size |
|---|---|
| Cylinder (Diameter) | 0.762 mm (0.030 in) |
| | 1.59 mm (0.0625 in) |
| | 2.31 mm (0.091 in) |
| Sandpaper | 40 GRIT |
| | 180 GRIT |
| | 1200 GRIT |
| | Sandpaper backing ~ 0.4 mm |
| Bluff shape | Smooth tape (0.5 mm) |

Table 2. Resultant uncertainties in experimental values

| Quantity | Uncertainty | Quantity | Uncertainty |
|---|---|---|---|
| $St$ | 4.0% | $U$ | 1.6% |
| $T$ | 0.1% (°C) | $u'$ | 7.1% |
| $uv$ | 11.9% | $vt$ | 21.0% |

*Boundary layer probes*

A single hot wire and a custom-made, three-sensor wire were used in this study to obtain estimates of velocity and temperature variation in the boundary layer. The single-wire boundary layer probe was a 4 micron tungsten wire configured in a standard TSI model 1218–T1.5. The three-sensor boundary layer probe consisted of two 2.5 $\mu$m, platinum-coated hot wires in an X-array operated in constant temperature modes and a platinum 1.2 $\mu$m cold wire operated in a constant current mode. Due to the extremely close spacing between the three sensors (0.35 mm), relatively low overheats were used during probe operation to limit "cross-talk" between the sensors. The two constant temperature sensors were operated with overheat ratios of 1.43 and 1.66, and the constant current sensor was operated at 0.1 mA. The three-sensor probe was used to measure local $u$, $v$ and $t$ variations simultaneously. The velocity and temperature signals were sampled at 2 kHz (analog low-pass filtered-cut-off frequency 1 kHz) for 20 s at each measurement location. Additional information concerning the probe design and qualification are given in Shome [22] and Wang *et al.* [23].

*Data reduction*

The surface heat transfer results presented in this paper are shown in terms of the local Stanton number. The fluid properties are evaluated at free-stream conditions, with corrections made for relative humidity effects. The heat flux to the free-stream was determined by subtracting the back loss, the radiation loss and the streamwise conduction loss from the measured power input. The energy balance described above, was applied to a $2.5 \times 2.5$ cm area of the 1.56 mm lexan layer of the test surface [see Fig. 1(c)]; then the surface temperature was calculated by correcting each measurement obtained from the thermocouples embedded in the test surface. The free-stream velocity was measured by using a micro-manometer connected to a Pitot tube. Finally, the free-stream temperature was measured by a calibrated thermocouple with corrections for recovery and compressibility effects. The methodology of heat transfer measurement outlined above and the associated uncertainty analysis was similar to those discussed in Wang and Simon [24]. A detailed uncertainty analysis was conducted by Pinson [25], using the procedure set forth by Kline and McClintock [26] and Moffat [27]. The resultant uncertainties are listed in Table 2.

The single hot wire and the X-array of hot wires in the three-sensor probe were corrected for the effects of varying temperature as suggested by Chua and Antonia [28]. The three-sensor probe was corrected by using instantaneous temperature fluctuations, and the single-wire probe measurements were corrected by using mean free-stream temperatures. Following the method of LaRue *et al.* [29], Wang, *et al.* [23] concluded that velocity correction of the cold wire in the three-sensor probe was unnecessary. Additional details on the data reduction process and the experimental procedure for this study are documented in Pinson [25].

## RESULTS AND DISCUSSION

*Undisturbed cases*

The surface heat transfer distributions (normalized in terms of the Stanton number and the local Reynolds number) of the undisturbed cases are shown in Fig. 3. The laminar and turbulent correlations, obtained from Kays and Crawford [30], presented in the figure compensate for the unheated starting length of a uniformly heated test surface, and are of the form

$$St_{\text{LAMINAR}} = 0.453 Pr^{-0.67} Re_x^{-0.5} \times \left[1 - \left(\frac{X_{\text{UHSL}}}{x}\right)^{0.75}\right]^{-0.333} \quad (1)$$

and

$$St_{\text{TURBULENT}} = 0.0287 Pr^{-0.4} Re_x^{-0.2} \times \left[1 - \left(\frac{X_{\text{UHSL}}}{x}\right)^{0.9}\right]^{-0.111}. \quad (2)$$

The initial portions of all the cases shown begin with a trend that follows the laminar unheated starting-length correlation, and then they deviate from the correlation at various Reynolds numbers, $Re_x$, because of the laminar-turbulent transition. The minimum local Stanton number for the 2.72 m s$^{-1}$ case occurs at an $Re_x$ of $2.24 \times 10^5$. Increasing the free-stream velocity, $U_\infty$ to 4.89 m s$^{-1}$ delays the onset of transition to an $Re_x$ of $3.59 \times 10^5$. The onset of transition for the undisturbed case is defined here as the location where $St$ reaches a minimum and starts to deviate from the

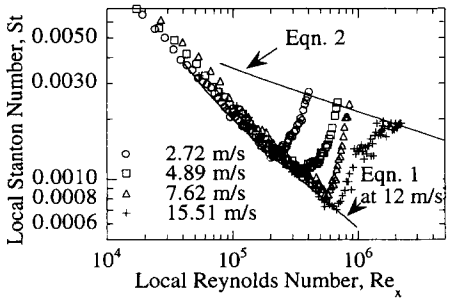


Fig. 3. Local surface heat transfer of the undisturbed case at various free-stream velocities.

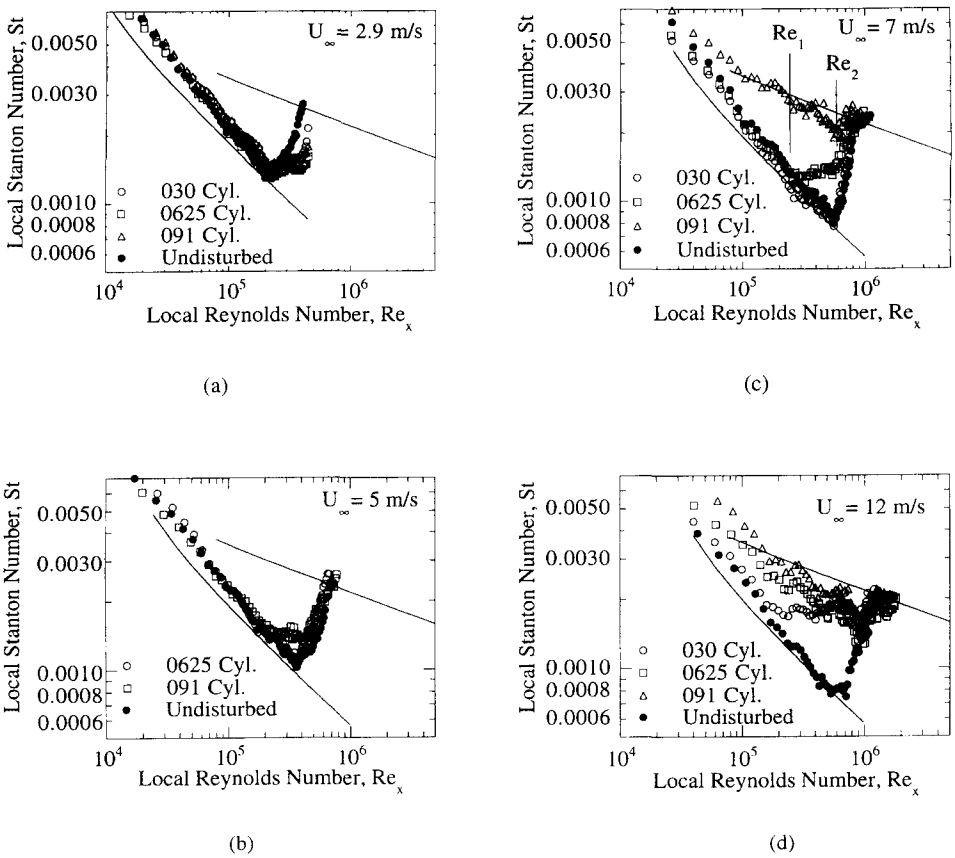


Fig. 4. Comparison of local Stanton number measurements between the undisturbed case and the cylinder leading edge conditions: (a) $U_\infty = 2.9$ m s$^{-1}$; (b) $U_\infty = 5$ m s$^{-1}$; (c) $U_\infty = 7$ m s$^{-1}$; (d) $U_\infty = 12$ m s$^{-1}$.

laminar correlation. This trend of delayed transition with increased $U_\infty$ continued until the free-stream velocity reached 15.5 m s$^{-1}$. The delay in the onset of transition between 2.72 and 15.5 m s$^{-1}$ is believed to be the result of decreasing free-stream turbulence intensity (FSTI), which was measured during the experiments. The FSTI of the 2.72 m s$^{-1}$ case is 1.1% and the FSTI of the 7.62 m s$^{-1}$ case is 0.4%.

Inaccuracies in the estimation of the radiant heat loss from the heated test surface could have caused the observed discrepancies between the laminar data and the laminar correlation. The emissivity (a value of 0.5 was used) of the heated test surface was the primary uncertainty in the radiant heat loss calculation. Although the deviation from the correlation is significant in the laminar region, the discrepancy does not affect the comparative nature of this study.

*Leading-edge roughness effects on heat transfer*

The surface heat transfer results from the various roughened leading-edge conditions (LECs) are shown with the undisturbed case in Figs. 4 and 5. Cylinder and sandpaper LECs do not affect the location of a transition onset at a $U_\infty$ of 2.9 m s$^{-1}$ [see Figs. 4(a) and 5(a)], but the effects of the LEC caused the slope of the $St$ distribution in the transition region to deviate from the undisturbed case. The similar distribution of the transitional data for the cases with sandpaper at the leading edge suggests that at this low free-stream velocity, the maximum roughness height, not the specific distribution of the roughness height, has the most significant effect on heat transfer. As the free-stream velocity increased, the $St$ distributions for the roughened LEC cases began to deviate more and more from the undisturbed case. Inspection of the figures suggests that the greater maximum roughness height produces greater deviation from the undisturbed $St$ distribution for a given free-stream velocity.

Several features of the Stanton number results of the cylinder LECs indicate a strong dependence on free-stream velocity. As mentioned earlier, the slowest free-stream velocity case (2.9 m s$^{-1}$) exhibited a milder slope in the transition regions of the roughened LEC cases than was seen in the transition region of the undisturbed case [Figs. 4(a) and 5(a)]. The slope of the transitional $St$ distributions for the 030 and 0625 cases more closely resembled the undisturbed case when $U_\infty$ was increased to 5 m s$^{-1}$ [Fig. 4(b)]. In the early transition region, the 091 cylinder case exhibited an unusual deviation from the undisturbed behavior when $U_\infty$ was 5 m s$^{-1}$. As shown in Fig. 4(b), a distinct departure from the undisturbed case began at an $Re_x$ of $2 \times 10^5$ until a $Re_x$ of $4 \times 10^5$ was reached, where the slope of $St$ becomes steeper and more like a typical

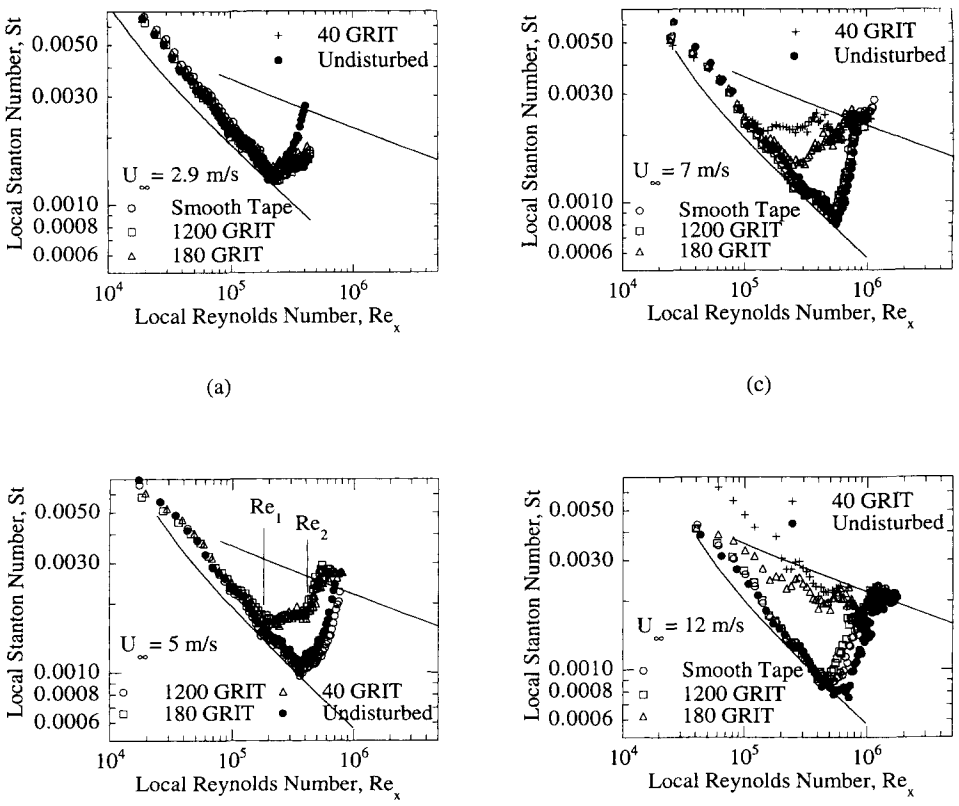


Fig. 5. Comparison of local Stanton number measurements between the undisturbed case and the sandpaper leading edge conditions: (a) $U_\infty = 2.9$ m s$^{-1}$; (b) $U_\infty = 5$ m s$^{-1}$; (c) $U_\infty = 7$ m s$^{-1}$; (d) $U_\infty = 12$ m s$^{-1}$.

transition. As shown in Fig. 4(c), the $St$ of the 091 cylinder case followed the turbulent correlation at $U_\infty = 7$ m s$^{-1}$; however, the $St$ distribution of the 0625 cylinder case at 7 m s$^{-1}$ [Fig. 4(c)] exhibited a dual-slope behavior similar to the behavior of the 091 case at 5 m s$^{-1}$ [Fig. 4(b)]. Although the 091 cylinder case shown in Fig. 4(c) approximately follows the turbulent correlation, an unexpected degree of waviness in the $St$ distribution was observed. The variation in the measured distribution was 6.4% above the correlation at an $Re_x$ of $1.88 \times 10^5$ and 22% below it at $6.09 \times 10^5$. Increasing $U_\infty$ to 12 m s$^{-1}$, as shown in Fig. 4(d), caused all three cylinder LECs to exhibit similar waviness in $St$. In the upstream region ($Re_x < 2 \times 10^5$), the $St$ distribution increased and shifted upwards with little change in slope as $U_\infty$ and the cylinder diameter increased. For the 091 cylinder case at 12 m s$^{-1}$, the magnitude of the $St$ distribution near the leading edge was similar to that of the turbulent $St$ correlation, but the slope was almost the same as the laminar correlation. The wavy behavior observed in the $St$ distribution of the 091 cylinder case and the dual-slope behavior in the transitional region of the 0.0625 cylinder case are examined in greater detail in subsequent sections of this discussion.

The $St$ behavior of the sandpaper LECs (Fig. 5) was similar to that shown by the cylinder LECs. The 40 GRIT case at a $U_\infty$ of 5 m s$^{-1}$ in Fig. 5(b) was the only sandpaper test case that exhibited the dual-slope behavior in the transitional $St$ data that was observed in two of the cylinder LECs, but the change in slope at an $Re_x$ of $4 \times 10^5$ was not as distinct as the change in the 091 cylinder case [Fig. 4(b)]. At a $U_\infty$ of 7 m s$^{-1}$ [Fig. 5(c)], the 40 GRIT and 180 GRIT cases exhibited laminar behavior until an $Re_x$ of $1.3 \times 10^5$ and $2 \times 10^5$ was reached, respectively. Then, both $St$ distributions began laminar-turbulent transition with waviness similar to that observed earlier in the higher speed cylinder LEC cases.

*Bluff leading-edge effect*

Smooth tape (0.5 mm thick) was used to investigate bluff leading-edge effects on $St$. The results at various speeds are shown in Fig. 5, together with the sandpaper LEC's. At a $U_\infty$ of 7 m s$^{-1}$, the $St$ distribution downstream of the bluff leading edge indicated that the onset of transition occurred at an $Re_x$ of $5.3 \times 10^5$ which is only 3% earlier than the onset for the undisturbed case. Increasing the $U_\infty$ to 12 m s$^{-1}$ caused the bluff leading edge condition to induce transition 15% earlier than the undisturbed case. Compared to the deviations induced by the sandpaper strips at this free-stream velocity, the bluff body effect of the sandpaper backing is relatively small.

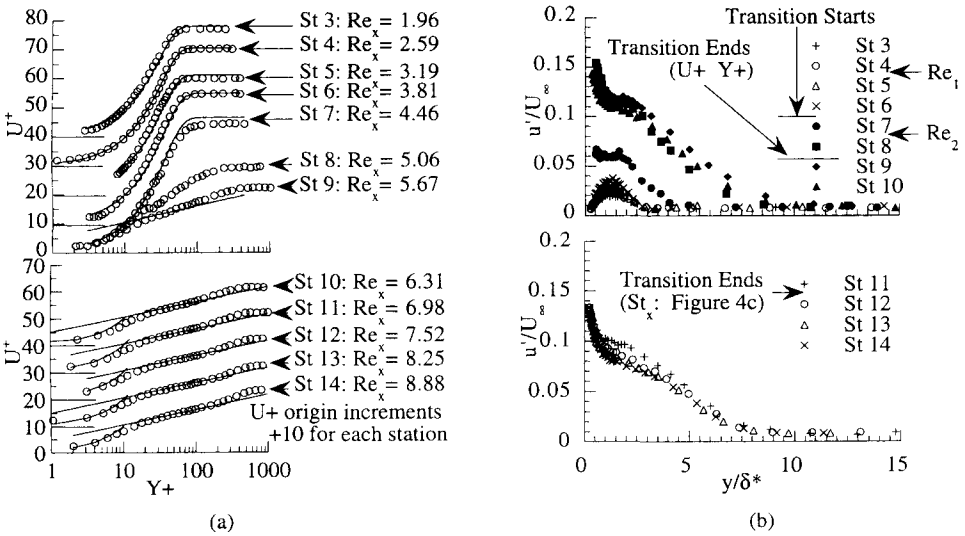


Fig. 6. Boundary layer profiles of the 0625 cylinder case ($U_\infty = 7$ m s$^{-1}$): (a) mean velocity profiles normalized in terms of local wall coordinates; $U^+$ and $Y^+$, Reynolds numbers are $\times 10^{-5}$; (b) $u'$ distribution.

*Dual-slope Stanton number behavior in transition region*

The 091 cylinder [Fig. 4(b)], the 40 GRIT sandpaper at 5 m s$^{-1}$ [Fig. 5(b)], and the 0625 cylinder at 7 m s$^{-1}$ [Fig. 4(c)] all exhibited the dual-slope behavior in $St$ between the laminar and turbulent correlations. Since this behavior was not observed in the undisturbed case and was not previously known to the authors, further study of the transport phenomena in the mean boundary layer was needed to provide insight into the physical mechanisms of the dual-slope region. Among these three similar cases, detailed measurements of the boundary layer of the 0625 cylinder case ($U_\infty = 7$ m s$^{-1}$) were obtained. The velocity profiles, normalized with respect to local wall coordinates, are shown in Fig. 6(a). The streamwise velocity profiles begin to significantly deviate from the Blasius correlation between an $Re_x$ of $4.46 \times 10^5$ and $5.06 \times 10^5$. During the wall heat transfer investigation, the local Stanton number began to deviate from the laminar correlation at an $Re_x$ of $2.88 \times 10^5$ (referred to as $Re_1$) and the slope of the $St$ distribution became steeper at an $Re_x$ of $4.88 \times 10^5$ (referred to as $Re_2$). The mean velocity profiles suggest that the boundary layer experienced transition only after $Re_x$ became greater than $Re_2$.

Further examination of the RMS quantities, $u'$, $\overline{uv}$, and $\overline{vt}$, verifies the laminar and transitional status in the dual-slope region. Inspection of the $u'$ profiles shown in Fig. 6(b) indicates that the $u'$ variations increased in amplitude between stations 3 and 6 (the range corresponding to $Re_1$ and $Re_2$) with maximum values of $u'/U_\infty$ ranging from 0.038 to 0.067, but the amplitude of the oscillations was still pre-transitional (typical maximum $u'/U_\infty$ value: 0.15). At station 7, the $u'/U_\infty$ distribution was relatively constant at 0.061 from a $y/\delta^*$ of 0.45–0.67. This wide, relatively flat ($\pm 5\%$ variation) region was not present in the undisturbed case (see Wang *et al.* [23]). Furthermore, the LEC caused the $u'$ profiles to continue developing in the early turbulent region of the boundary layer (the maximum station-to-station variation is an average of 8% downstream of station 10), even though the mean velocity profiles indicated fully developed turbulent flow in this region [see Fig. 6(a)]. The $\overline{uv}$ profiles depicted in Fig. 7(a) also show negligible activity in generating Reynolds shear stress between stations 4 and 6 ($\overline{uv}/U_1^2$ less than 0.08), indicating pre-transitional flow in the region $Re_1$ to $Re_2$. Large amplifications indicative of transitional flow were observed downstream of $Re_2$ ($\overline{uv}/U_1^2$ greater than 0.8). Similar to the $u'$ profiles, the $\overline{uv}$ profiles continued to develop in the early turbulent portion of the boundary layer. The $\overline{vt}$ profiles shown in Fig. 7(b), exhibit behavior similar to $\overline{uv}$ throughout the streamwise boundary layer development, and exhibit negligible Reynolds heat flux transport in the region between $Re_1$ and $Re_2$.

The instantaneous velocity signals were inspected to provide more information about flow behavior in the dual-slope region. Representative velocity signals taken around $Y^+ = 10$ at various stations for the 0625 cylinder case are shown in Fig. 8. The velocity signals of those stations between $Re_1$ and $Re_2$ (stations 5 and 6) are laminar-like with sinusoidal-like oscillations. However, the velocity traces of stations 7 and 8, which bracket $Re_2$, show intermittent turbulent/nonturbulent behaviour, which undoubtedly indicates transitional flow. Similar behavior was observed for a low-speed 40 GRIT sandpaper case at $U_\infty = 5$ m s$^{-1}$.

These boundary layer results suggest that a roughened leading edge may produce a pre-transitional region where the momentum and thermal transports in the boundary layer behave like laminar flow; however, the wall heat transfer significantly deviates from the laminar correlation.

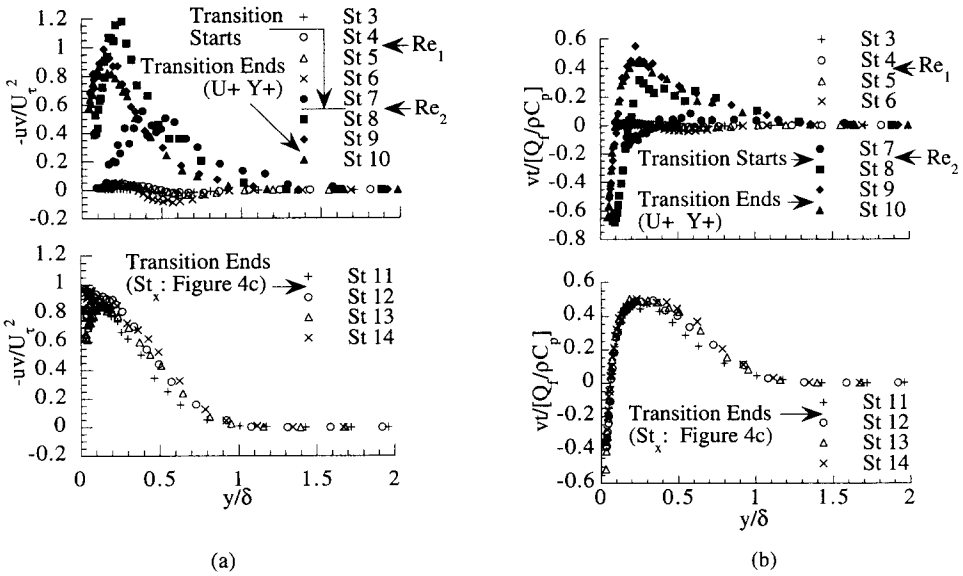


Fig. 7. Boundary layer profiles of the 0625 cylinder case ($U_\infty = 7$ m s$^{-1}$) continued: (a) Reynolds shear stress distribution; (b) Reynolds heat flux distribution.

*Waviness in heat transfer data*

The results of the Stanton number distributions show that waviness is present in high-speed cases with roughened leading edges. Inspection of Figs. 4 and 5 indicates that rougher leading-edge conditions cause significant wavy *St* behavior at lower free-stream velocities. Since the waviness was not observed in the undisturbed case, it was reasoned that the waviness was most likely induced by the flow disturbances introduced by the roughened leading edge.

The waviness could also have been caused by problems with the experimental apparatus and the test surface. Tests conducted at a fixed free-stream velocity (15 m s$^{-1}$) with varying power input levels indicate that the degree of waviness was not a function of power input. In addition, the test surface was qualified by conducting a convective heat transfer test in a laminar flow with mild acceleration of $K \sim 4 \times 10^{-8}$. The mild acceleration was caused by the boundary layer growth in a constant-area channel. The *St* data of this qualification test matched the laminar correlation and no waviness was observed. The closeness of the match indicates that the heat flux out of the test surface was reasonably uniform and that all of the thermocouples embedded in the test surface functioned well. The energy balance used to determine the *St* distribution indicates that losses through the back of the heated wall were less than 1% of the flux to the free-stream. Hence, even an order of magnitude error in back-loss calculations would not have affected the magnitude of the heat flux to the free-stream to such an extent that could account for the degree of waviness present in the Stanton number data. A more detailed discussion of the waviness behaviors is presented in Pinson [25].

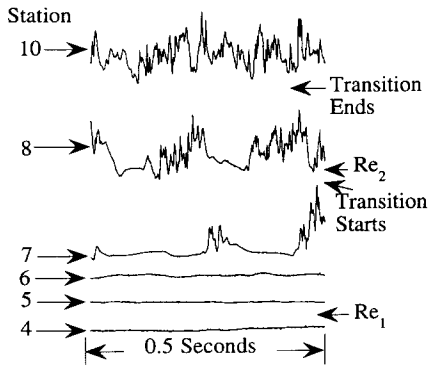


Fig. 8. Instantaneous velocity signals around $Y^+ = 10$ at various streamwise locations for the 0625 cylinder case ($U_\infty = 7$ m s$^{-1}$).

With the removal of the experimental apparatus and the test surface as possible culprits for the waviness, it seems possible that the observed waviness could be the result of nonlinear instabilities brought on by the finite amplitude disturbance introduced at the leading-edge. These nonlinearities in the flow condition could make the boundary layer sensitive to the minor geometrical variations present in the test section in such a way that the actual form or characteristic that causes the disturbance becomes unimportant. These minor surface disturbances, whatever they are, seem to be amplified as the free-stream velocity increases, and they significantly affect the heat transfer pattern downstream.

This study intentionally isolated the effects of leading-edge roughness on downstream flow and heat transfer behavior, so the test surface downstream of the leading-edge roughness was made smooth and flat. To better simulate the roughness condition of an in-service turbine blade, further studies are being undertaken by the authors to investigate the interactive

effects of leading-edge roughness with the downstream roughness.

## CONCLUSIONS

A total of eight leading-edge conditions were examined to determine their effect on laminar-turbulent flow transition and downstream heat transfer flow behavior. In order to simulate the randomly distributed roughness located near the leading edge of the turbine blade, 1200, 180 and 40 GRIT sandpaper strips were adhered to the leading edge of the test surface. Similarly, 0.762, 1.59 and 2.31 mm diameter cylinders were chosen to simulate the relatively isolated peak nature of the roughness structure. Tests were also conducted by using a smooth strip of tape at the leading edge to determine the relative effects of the sandpaper backing and the actual roughness of the sandpaper. All of these leading-edge conditions were compared to the undisturbed leading edge.

Overall, greater maximum roughness height was observed to induce greater enhancement of the surface heat transfer than the undisturbed case. Depending on the free-stream velocity and the distance from the leading edge disturbance, the enhancement ranged from negligible to 200%. At low free-stream velocities ($U_\infty = 5$ m s$^{-1}$), the maximum roughness height was the primary contributor to deviations observed from the undisturbed case, irrespective of the roughness geometry. At higher free-stream velocities, 5–7 m s$^{-1}$, the cases employing the 091 cylinder LEC, 0625 cylinder LEC and the 40 GRIT sandpaper exhibited a dual-slope region between the laminar and turbulent $St$ vs $Re_x$ correlations. Although the first slope was significantly different from the laminar correlation (as much as 88% higher), inspection of the mean velocity profiles, RMS fluctuations, Reynolds shear stress and instantaneous velocity signals indicated that the boundary layer was pre-transitional in this region. The second segment of the dual-slope $St$ distribution was steeper than the first and the junction between these two segments was determined to be the approximate onset of boundary layer transition. For greater roughness, wavy $St$ distributions were observed at higher free-stream velocities.

The presence of the dual-slope and wavy $St$ behavior in some of the roughened leading-edge cases suggests that heat transfer is sensitive to leading-edge effects. In each situation, the behavior seems to be the result of nonlinear amplification introduced by finite disturbances at the leading edge. These nonlinear waves tend to amplify minor disturbances on the surface which propagate downstream in such a way that the wall heat transfer pattern is significantly affected. However, additional study of both of these behaviors is required before the mechanisms causing these behaviors can be understood.

*Acknowledgements*—This program was funded by the College of Engineering at Clemson University. The experiments were performed in the test facilities sponsored by a grant from the Air Force Office of Scientific Research (Grant No. F49620-94-1-0126).

## REFERENCES

1. Mayle, R. E., The role of laminar-turbulent transition in gas turbine engines. *Journal of Turbomachinery*, 1991, **113**, 509–537.
2. Hodson, H. P., Huntsman, I. and Steele, A. B., An investigation of boundary layer development in a multistage LP turbine, 93-GT-310, ASME, 1993.
3. Taylor, R. P., Surface roughness measurement on gas turbine blades. *Journal of Turbomachinery*, 1990, **112**, 175–180.
4. Boynton, J. L., Tabibzadeh, R. and Hudson, S. T., Investigation of rotor blade roughness effects on turbine performance. *Journal of Turbomachinery*, 1993, **115**, 614–620.
5. Blair, M. F., An experimental study of heat transfer in a large-scale turbine rotor passage. *Journal of Turbomachinery*, 1994, **116**, 1–13.
6. Fage, A. and Preston, J. H., On transition from laminar to turbulent flow in the boundary layer. *Proceedings of the Royal Society of London*, 1941, **178**, 201–227.
7. Dryden, H. L., Review of published data on the effect of roughness on transition from laminar to turbulent flow. *Journal of the Aeronautical Sciences*, 1953, **20**, 477–482.
8. Klebanoff, P. S. and Tidstrom, K. D., Mechanism by which a two-dimensional roughness element induces boundary-layer transition. *Physics of Fluids*, 1972, **15**, 1173–1188.
9. Jacobs, W., Variation in velocity profiles with change in surface roughness of boundary. Technical Memorandum 951, NACA, 1940.
10. Klebanoff, P. S. and Diehl, Z. W., Some features of artificially thickened fully developed turbulent boundary layers with zero pressure gradient. Report 1110, NACA, 1951.
11. Antonia, R. A. and Luxton, R. E., The response of a turbulent boundary layer to a step change in surface roughness: Part 1. Smooth to rough. *Journal of Fluid Mechanics*, 1971, **48**, 721–761.
12. Antonia, R. A. and Luxton, R. E., The response of a turbulent boundary layer to a step change in surface roughness: Part 2. Rough to smooth. *Journal of Fluid Mechanics*, 1972, **53** (Part 4), 737–757.
13. Andreopoulos, J. and Wood, D. H., The response of a turbulent boundary layer to a short length of surface roughness. *Journal of Fluid Mechanics*, 1982, **118**, 143–164.
14. Ligrani, P. M., Moffat, R. J. and Kays, W. M., Artificially thickened turbulent boundary layers for studying heat transfer and skin friction on rough surfaces. *Journal of Fluids Engineering*, 1983, **105**, 146–153.
15. Taylor, R. P., Hosni, M. H. and Coleman, H. W., Comparison of constant wall temperature and heat flux cases for the turbulent rough-wall boundary layer. *Experimental Heat Transfer*, 1990, **3**, 117–127.
16. Taylor, R. P., Taylor, J. K., Hosni, M. H. and Coleman, H. W., Heat transfer in the turbulent boundary layer with a step change in surface roughness. 91-GT-266, ASME, 1991.
17. Keller, F. J., Flow and thermal structures in heated transitional boundary layers with and without streamwise acceleration. Ph.D. thesis, Department of Mechanical Engineering, Clemson University, Clemson, South Carolina, 1993.
18. Kuan, C. L., An experimental investigation of intermittent behavior in the transitional boundary layer. M.S.

thesis, Department of Mechanical Engineering, Clemson University, Clemson, South Carolina, 1987.
19. Zhou, D., Effects of elevated free-stream turbulence and streamwise acceleration on flow and thermal structures in transitional boundary layers. Ph.D. thesis, Department of Mechanical Engineering, Clemson University, Clemson, South Carolina, 1993.
20. Elovic, E., Personal Communication, General Electric Aircraft Engines, Cincinnati, OH, 1992.
21. Tarada, F. H. A., Heat transfer to rough turbine blading. Ph.D. thesis, University of Sussex, England, 1987.
22. Shome, B., Development of a three-wire probe for the measurement of Reynolds stresses and heat fluxes in transitional boundary layers. M.S. thesis, Department of Mechanical Engineering, Clemson University, Clemson, South Carolina, 1991.
23. Wang, T., Keller, F. J. and Zhou, D., Experimental investigation of Reynolds shear stresses and heat fluxes in a transitional boundary layer. *Journal of Experimental Fluid and Thermal Science*, 1992, **12**, 352–363.
24. Wang, T. and Simon, T. W., Development of a special-purpose test surface guided by uncertainty analysis. *Journal of Thermophysics*, 1989, **3**, 19–26.
25. Pinson, M., The effects of initial conditions on heat transfer in transitional boundary layers. M.S. thesis, Clemson University, Clemson, South Carolina, 1991.
26. Kline, S. J. and McClintock, Describing uncertainties in single-sample experiments. *Mechanical Engineering*, 1953, **75**, 3–8.
27. Moffat, R. J., Contributions to the theory of single-sample uncertainty analysis. *Journal of Fluids Engineering*, 1982, **104**, 250–260.
28. Chua, L. P. and Antonia, R. A., Turbulent Prandtl number in a circular jet. *International Journal of Heat and Mass Transfer*, 1990, **33**, 331–339.
29. LaRue, J. C., Deaton, T. and Gibson, C. H., Measurement of high-frequency temperature. *Review of Scientific Instruments*, 1975, **46**, 757–764.
30. Kays, W. M. and Crawford, M. E., *Convective Heat and Mass Transfer*, 3rd edn. McGraw-Hill, New York, 1993, pp. 175, 179 and 281.